Thermochimica Acta, 162 (1990) 367–373
Elsevier Science Publishers B.V., Amsterdam – Printed in The Netherlands

DEVITRIFICATION STUDIES OF VARIOUS PbO-CONTENT $PbO-B_2O_3-ZnO$ GLASS SYSTEMS

JINN-SHING LEE, JAW-CHAY PERNG and CHING-WANG HUANG

Department of Chemistry, Chung Yuan Christian University, Chung-Li, 32023 Taiwan

(Received 3 November 1989)

ABSTRACT

The devitrification mechanisms of seven $PbO-B_2O_3-ZnO$ glasses were studied using non-isothermal techniques and/or by comparing the exothermic peak temperatures of the fine glass powder and the coarse glass powder on the DTA curves. Experimental results suggest that the devitrification mechanism of lower PbO content $PbO-B_2O_3-ZnO$ glasses is almost surface nucleation dominated, but surface nucleation controlled by both diffusion and bulk nucleation occurs in higher PbO-content $PbO-B_2O_3-ZnO$ glasses.

INTRODUCTION

The binary system $PbO-B_2O_3$ gives a broad series of glasses. At higher lead contents the glasses devitrify too rapidly for most purposes, but provide the lowest melting glass solder. The effect of adding ZnO to the $PbO-B_2O_3$ glasses is to give desirable solder glass, although the amount of ZnO that can be used is limited by the tendency of these glasses to devitrify. This effect begins near 5% ZnO and increases rapidly with ZnO content until at 20% and above [1] the glasses become unsuitable. Most solders containing less than 20% ZnO give satisfactory wetting, even if partial devitrification occurs.

TABLE 1

Weight% compositions of $PbO-B_2O_3-ZnO$ glasses

Glasses	PbO	B_2O_3	ZnO
A	60	20	20
B	65	20	15
C	70	15	15
D	70	10	20
E	75	10	15
F	80	10	10
G	85	10	5

In this study, the glass compositions investigated are given in Table 1. A non-isothermal technique was applied in order to calculate the devitrification mechanism and the kinetic parameters of crystal growth of the PbO–B_2O_3–ZnO glasses.

EXPERIMENTAL

Samples of PbO–B_2O_3–ZnO glasses were prepared by melting the pure reagents in a platinum crucible in an electric furnace and casting them in graphite moulds at a high cooling rate. The quenched glasses were crushed very carefully using a stainless steel pestle and mortar, and then sieved in order to obtain a coarse powder between 30 and 50 mesh. The glass powder below 50 mesh was ground again in an agate mortar, and then sieved in order to obtain very fine (−325 mesh) particles. No crystalline phases were detected by X-ray diffraction of the quenched glasses. Differential thermal analysis (DTA) of 30 mg of the fine glass powder and the coarse glass powder was performed in air with heating rates of 1–20 °C min^{-1}. A Rigaku–Denki differential thermal analyser, model 8121, was used and α-Al_2O_3 powder was used as reference material.

RESULTS AND DISCUSSION

The non-isothermal devitrification of glasses is well described by the Johnson–Mehl–Avrami (JMA) equation [2,3,4]

$$-\ln(1-\alpha) = (kt)^m \qquad (1)$$

The rate constant, k, is related to the absolute temperature, T, by an Arrhenius-type equation

$$k \propto A \exp(-E/RT) \qquad (2)$$

where α is the volume fraction of devitrified phase at time t, E represents the overall kinetic barrier to devitrification and A is a constant. The parameter m depends on the mechanism and morphology of devitrification. It is evident from the DTA curves that m allows a distinction to be made only in straightforward cases; if we consider that devitrification is controlled by the reaction at the glass–crystal interface, ranges m from 1, for one-dimensional devitrification (or devitrification from surface nuclei), to 3 for three-dimensional devitrification. For the diffusion-controlled devitrification the corresponding m-range is 0.5–1.5.

As the devitrification of a glass proceeds, the heat of devitrification is evolved and an exothermic peak appears on the DTA curve. If the degree of devitrification reaches the same specific value independent of the heating

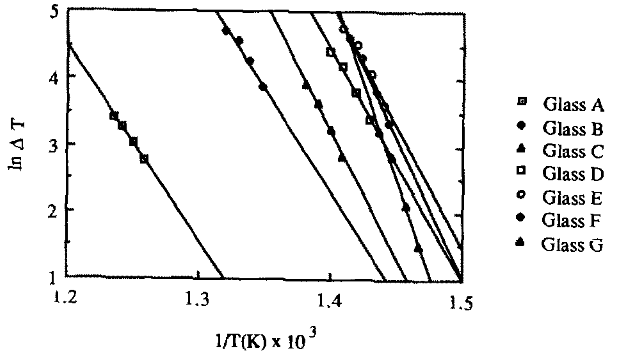

Fig. 1. Plot of ln ΔT against $1/T$ used to determine the value of mE_g for coarse glass powder.

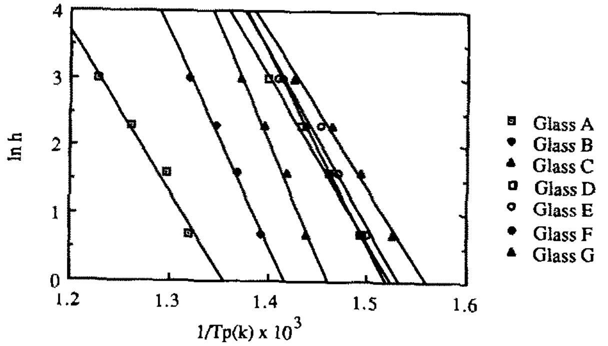

Fig. 2. Plot of ln h against $1/T_p$ used to determine the activation energy for crystallization of coarse glass powder by heating rate.

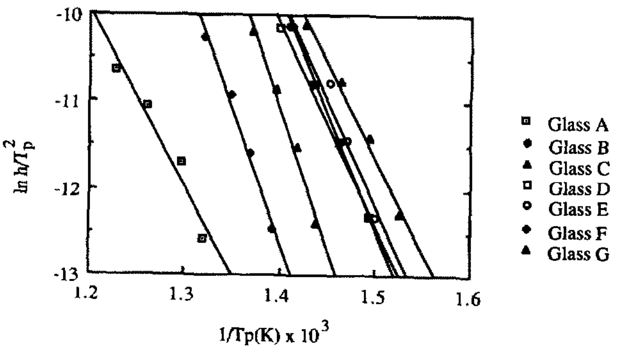

Fig. 3. Plot of ln h/T_p^2 against $1/T_p$ used to determine the activation energy for crystallization of coarse glass powder by heating rate.

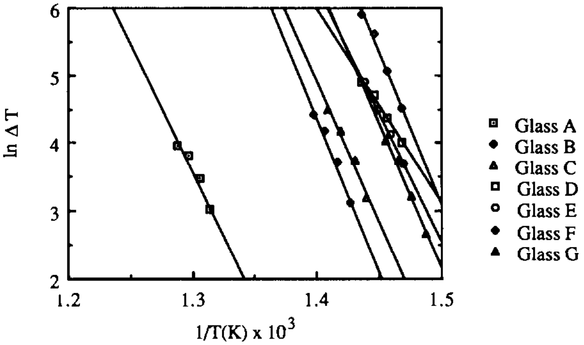

Fig. 4. Plot of ln ΔT against $1/T$ used to determine the value of mE_g for fine glass powder.

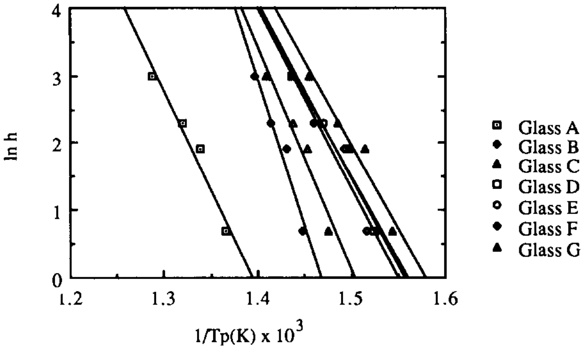

Fig. 5. Plot of ln h against $1/T_p$ used to determine the activation energy for crystallization of fine glass powder by heating rate.

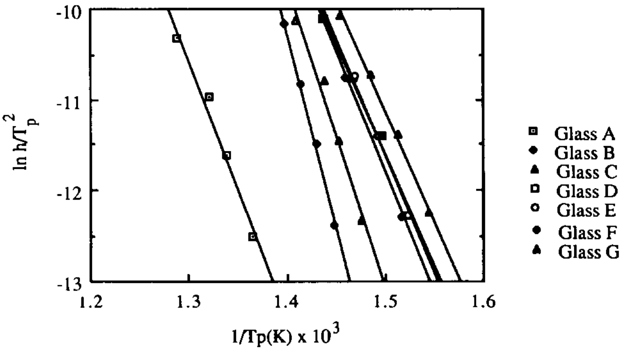

Fig. 6. Plot of ln h/T_p^2 against $1/T_p$ used to determine the activation energy for crystallization of fine glass powder by heating rate.

TABLE 2

Non-isothermal kinetic data for coarse powdered PbO–B_2O_3–ZnO glasses

Glasses	E_1 [a] (kJ mol^{-1})	E_2 [b] (kJ mol^{-1})	E_{avg} (kJ mol^{-1})	mE (kJ mol^{-1})	m
A	197.69	167.78	182.76	234.51	1.28
B	265.22	253.30	259.28	281.83	1.09
C	282.00	270.20	276.10	316.27	1.15
D	203.76	192.21	197.99	256.90	1.30
E	212.42	200.87	206.65	309.03	1.50
F	236.35	218.15	227.27	375.35	1.65
G	194.14	179.16	186.65	322.25	1.73

[a] E_1, Activation energy calculated by plotting ln h versus $1/T_p \times 10^3$.

[b] E_2, Activation energy calculated by plotting ln h/T_p^2 versus $1/T_p \times 10^3$ (Kissinger method).

rate (h), and if the deflection from the baseline (ΔT) is proportional to the instantaneous reaction rate, especially in the initial part of the exothermic peak, the change in temperature has a much larger effect on the deflection (ΔT) i.e. $\Delta T = C_1\ (\mathrm{d}\alpha/\mathrm{d}t)$. Then during a DTA run, the time of heating (t) at each temperature can be taken to be proportional to the reciprocal of the heating rate (h), if the latter is linear, i.e. $t = C_2\ (1/h)$, and C_1 and C_2 are constants.

The kinetic parameters can be calculated from the DTA curves using the following equations [5–7]

$$\ln \Delta T = -mE/RT + \text{constant} \qquad (3)$$

$$\ln h = -E/RT_p + \text{constant} \qquad (4)$$

$$\ln h/T_p^2 = -E/RT_p + \text{constant} \qquad (5)$$

Plotting ln ΔT against $1/T$ as shown in Figs. 1 and 4, ln h against $1/T_p$, Figs. 2 and 5 and ln h/T_p^2 against $1/T_p$, Figs. 3 and 6, gives straight lines in

TABLE 3

Non-isothermal kinetic data for fine powdered PbO–B_2O_3–ZnO glasses

Glasses	E_1 [a] (kJ mol^{-1})	E_2 [b] (kJ mol^{-1})	E_{avg} (kJ mol^{-1})	mE (kJ mol^{-1})	m
A	251.04	238.53	244.81	314.76	1.29
B	371.96	360.24	364.22	403.04	1.11
C	287.98	276.52	282.25	346.60	1.23
D	214.97	203.34	209.16	237.02	1.13
E	225.98	214.89	220.45	321.00	1.46
F	229.79	224.81	227.32	346.35	1.52
G	213.26	201.92	207.61	353.17	1.70

[a] E_1, Activation energy calculated by plotting ln h versus $1/T_p \times 10^3$.

[b] E_2, Activation energy calculated by plotting ln h/T_p^2 versus $1/T_p \times 10^3$ (Kissinger method).

all cases. The values of the kinetic parameters E and m were calculated from the slopes and are reported in Tables 2 and 3.

The values of m suggest that surface devitrification or surface devitrification controlled by diffusion takes place in the glasses in which the PbO content is lower than 75% by weight ($m < 1.5$), but bulk devitrification controlled by both diffusion and interfacial effects occurs in the glasses in

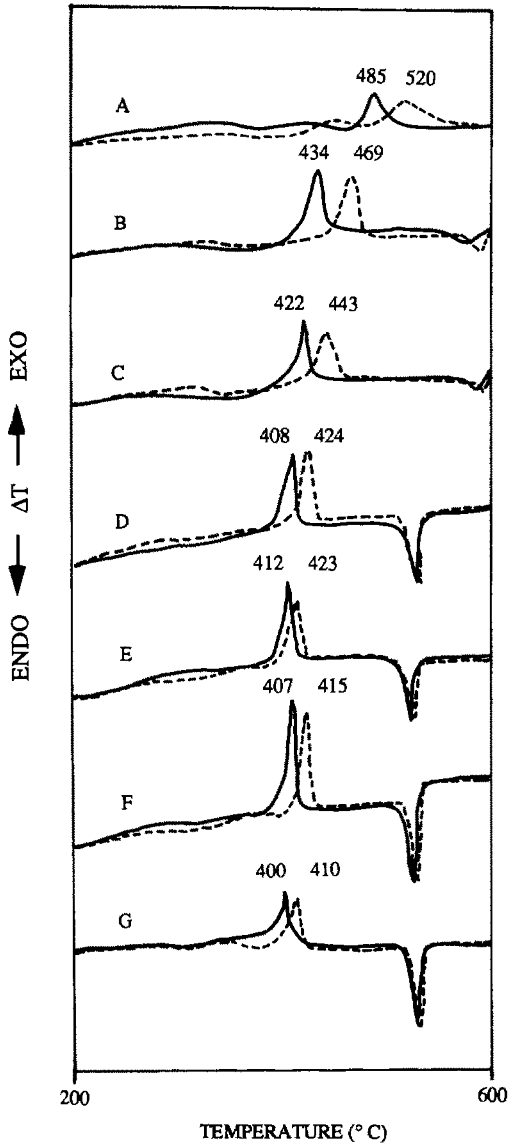

Fig. 7. Thermograms of coarse and fine glass powders. The solid lines represent −325 mesh powder, and the dashed lines powder between 30 and 50 mesh.

which the PbO content is higher than 75% by weight ($m \geq 1.5$). These results are consistent with the following demonstration.

To determine whether the devitrification begins at the surface or in the bulk of these glasses [8], we recorded thermograms for coarse and fine particles. For the glasses with PbO content lower than 75% by weight, the devitrification peak occurs at a considerably higher temperature for coarse particles than for fine, see Fig. 7A–D: this result indicates surface devitrification. For the glasses with PbO content higher than 75% by weight, however, the peaks were very close, see Fig. 7E–G, indicating bulk devitrification or, more appropriately, devitrification at the internal interface of the glass.

CONCLUSIONS

From the experimental results the following conclusions can be drawn.

(a) The non-isothermal method of comparing the exothermic peak temperatures of the DTA curves of coarse and fine glass powders is valid and useful for studying the devitrification nucleation mechanism.

(b) The devitrification mechanism of $PbO–B_2O_3–ZnO$ glass was changed by increasing the PbO content; in the lower PbO-content $PbO–B_2O_3–ZnO$ glasses, the devitrification takes place on the surface, but bulk devitrification occurs in the higher PbO-content $PbO–B_2O_3–ZnO$ glasses.

REFERENCES

1 R.H. Dalton, J. Am. Ceram. Soc., 39 (1956) 109.
2 F. Brandaï, A. Buri and A. Marotta, Thermochim. Acta, 120 (1987) 217.
3 D.R. Macfarlane, M. Matecki and M. Poulain, J. Non-Cryst. Solids, 64 (1984) 351.
4 A. Marotta, S. Saiello, F. Branda and A. Buri, Thermochim. Acta, 46 (1981) 123.
5 A. Marotta and A. Buri, Thermochim. Acta, 25 (1987) 155.
6 T. Ozawa, Polymer, 12 (1971) 150.
7 H.E. Kissinger, J. Res. Nat. Bur. Stand., 57 (1956) 217.
8 A.H. Kumar and R.R. Tummla, Am. Ceram. Soc. Bull., 57 (1978) 738.